

Structural and mechanical relaxation on annealing in glass-metal layered composites

M.A. Barbotko , O.N. Lyubimova , M.V. Ostanin 

Far Eastern Federal University, Vladivostok, Russia

✉ barbotko_ma@dvfu.ru

Abstract. The technological modes of annealing of the layered glass-metal composite material – glass-metal composite – which include heating-up to the glass softening point and aftercooling with annealing are investigated. The mathematical model of stress evolution is considered. The complexity in modeling is caused by the combined deformation of the glassy layer and the elastic-plastic layer with non-uniform temperature changes. Structural and mechanical relaxation processes in the glass transition interval are described within the framework of the relaxation kinetic theory of glass transition. The algorithm for calculations of technological and residual stresses in glass-metal composite, at different modes, is proposed. A comparison of the numerical method with the analytical solution obtained for constant thermomechanical parameters of materials is presented. The practical implications are in the possibility of modeling technological and residual stresses in laminated structural cylindrical systems functioning during cyclic heating-cooling to high temperatures, including glass transition and plastic deformation of the layers.

Keywords: glass-metal composite; structural and mechanical relaxation

Acknowledgements. *The reported study was funded by FEFU, project number 22-07-01-007.*

Citation: Barbotko MA, Lyubimova ON, Ostanin MV. Structural and mechanical relaxation on annealing in glass-metal layered composites. *Materials Physics and Mechanics*. 2023;51(4): 118-129. DOI: 10.18149/MPM.5142023_11.

Introduction

Advanced approaches to the simulation of new materials stand out the tendency of producing materials that combine the properties of glass and metal, which are called glass-metal composites: bioactive glass coatings in biomedicine [1], glass microspheres reinforced metal matrix [2–3], glass-metal nanocomposites, layered structural materials based on metal and glass fabric [4–6] or glass monolayers [7–8]. Manufacturing of glass-metal composites based on glass and metal monolayers is associated with heat treatment, during which glass layers are brought to a viscous liquid state, and then during cooling due to the difference in thermal coefficients of expansion, certain compressive stresses are formed in them, which are the reason for increasing the strength of glass layers.

The formulation of the mathematical model forecasting the mechanical behavior of the material with due regard to the glass transition process and plastic yield in metal in the course of heat treatment is essential.

The studies of the glass transition phenomenon have not yet allowed to develop a general theoretical understanding of the process, there are several basic theoretical approaches, among which the relaxation theory (transition theory within the two-state model) stands out as the most

experimentally tested one [10–12]. In the relaxation theory, glass transition is modeled as a transition of a medium from equilibrium (liquid) state to metastable (glassy) state through the change of a structural parameter characterizing the system state - "fictitious" temperature T_f [12–17]. The methods of calculating stresses in the course of heat treatment of, for example, flat leak-proof two-layered soldered joints of glass with metal, which are effectively used for calculations of stresses in amorphous coatings, are known [18–20]. Meantime, in the course of the glass-metal composite manufacture, the development of the elastoplastic strenuously-deformed state (in metal) resulting sometimes in destruction of the metal layer in case of mismatched parameters of the technological process and dimensions of metal layer is possible. The attempts to describe a change in the geometry of soldered joints under consideration and elastoplastic deformation of the metal element of a soldered joint require complication of the problem and adjustment of calculation methods of stress relaxation when passing through the glass transition interval, which determines the objective of this paper.

Statement of the Problem and mathematical model

The thermal regime of manufacturing the glass-metal composite (Fig. 1(a)) includes intervals of heating-up I_a , exposure I_b , cooling I_c and annealing, which is carried out either immediately at the cooling stage and associated with control of the rate of temperature change and exposure at the glass transition temperature or on reheating I_a^0 and following stages of controlled cooling I_b^0 and I_c^0 . Simulation of controlled cooling is necessary for monitoring and regulating of technological and residual stresses. On cooling from a temperature which can coincide with the glass-melting temperature or be not so many as it, the structure and properties of the glass change continuously. Such process is termed as glass transition, and it proceeds in certain interval (T_g^-, T_g^+) (Fig. 1(b)). The average temperature of the glass transition interval is referred the glass transition temperature T_g . The position of glass transition interval depends on the cooling rate and the prehistory of temperature treatment while the boundaries of glass transition interval T_g^- and T_g^+ are usually associated with those of hysteresis loop characterizing change of enthalpy under uniform cooling and heating-up from the equilibrium condition of the liquid melt to the frozen structure.

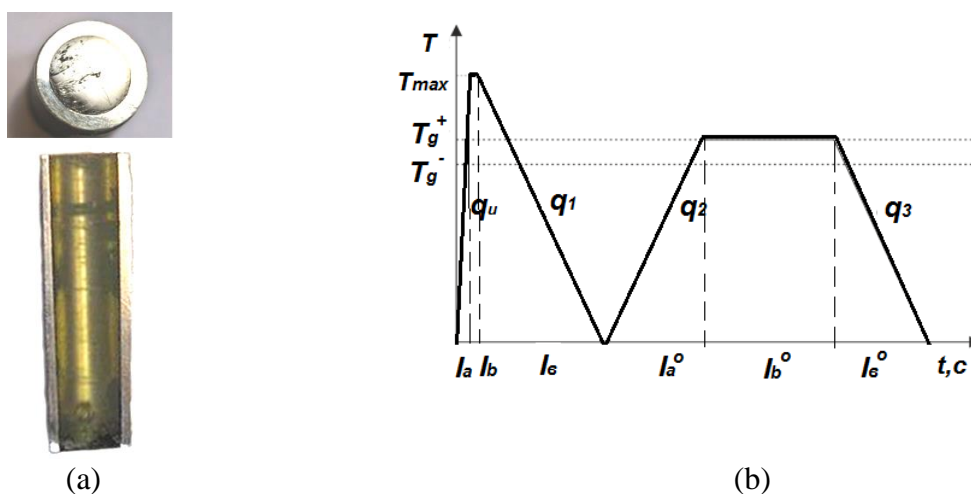


Fig. 1. Photographs of the experimental samples (a); temperature conditions of annealing (b)

When passing through the glass transition interval, the specificity of structure change, and mechanical relaxation is described by changing the fictitious (structural) temperature and the rate of its change relative to temperature, an analytical expression in the form of the Tule-Nayaranaswamy-Moynihan formula [13–15]:

$$T_f = T_0 + \int_0^t (1 - M_s(\xi - \xi')) \frac{dT}{d\xi'} d\xi', \quad (1)$$

here $T_0 = T_{\max}$, the function of the structural relaxation of glass properties is well described by the function of Kohlrausch [18]:

$$M_s(\xi) = e^{-(\xi/\tau_r)^b} = e^{-(\xi K_r/\eta_r)^b}, \quad (2)$$

where b is a constant for the glasses having fixed compositions ($0 < b < 1$), ξ is a "true" time, which being a temperature-invariant characteristic of viscoelastic properties, can be written as

$$\xi(t) = \int_0^t \frac{\eta_r}{\eta(t')} dt', \quad \text{where } \eta_r \text{ — shearing viscosity at arbitrarily chosen comparison temperature } T_r,$$

$\eta(t)$ — is current viscosity, $K_r = \eta_r/\tau_r$, τ_r — is relaxation time at the comparison temperature.

The analytical dependences of the change in viscosity and the thermal coefficient of linear expansion can be written as (3) and (4) commonly used for calculating thermal stresses in the flat soldered joint of glass with metal in the algorithm called "IHS calculation method (Institute of Silicate Chemistry)".

$$\lg \frac{\eta}{\eta_0} = B_e (T_f^{(-1)} - T_0^{(-1)}) + B_f (T^{(-1)} - T_f^{(-1)}), \quad (3)$$

$$\alpha = \alpha_e + (\alpha_f - \alpha_e) \left(\frac{dT_f}{dT} \right), \quad (4)$$

where η_0 is viscosity at T_0 , $B_e, \alpha_e, B_f, \alpha_f$ are coefficients characterizing the temperature dependences of η and α under conditions of the equilibrium and frozen structures, respectively.

The change of fictitious temperature (1), its rate and physical and chemical properties of liquid glass melt (2)-(4) during temperature treatment is determined from the solution of the heat and mass transfer problem, which is considered in work [21] for different methods of heating and cooling.

In mathematical simulation of the evolution of stresses in the glass-metal composite, different ways of thermomechanical deformation of the materials of which it composes – thermo-visco-plastic one with structural changes in the glass component and thermo-elastic-plastic one in the metal were taken into account. Simulation has been performed for a specific geometry representing composite stems: a glassy core and a steel shell. Assuming an axisymmetric, uniform heating along generatrix at small deformations in the cylindrical coordinate system, the components of the displacement tensor can be written in the form of the following unknown functions: $u_r = u(r, t)$, $u_\varphi = 0$, $u_z = w(z, t)$, and deformation tensors has

$$\text{a diagonal form and the components: } \varepsilon_{rr} = \frac{\partial u}{\partial r}, \quad \varepsilon_{\varphi\varphi} = \frac{u}{r}, \quad \varepsilon_{zz} = \frac{\partial w}{\partial z} = \varepsilon_z(t), \quad \varepsilon_{r\varphi} = \varepsilon_{rz} = \varepsilon_{\varphi z} = 0.$$

Equations of state for glass can be described on the basis of the Boltzmann-Volterra superposition principle [22] and the absence of bulk relaxation properties condition

$$s_i = 2G \left(e_i - \int_0^t M(\eta(t, t')) e_i dt' \right), \quad i = r, \varphi, z, \quad (5)$$

$$\sigma(r, t) = 3K\theta, \quad (6)$$

here $\sigma = (\sigma_r + \sigma_\varphi + \sigma_z)/3$, $\varepsilon = (\varepsilon_r + \varepsilon_\varphi + \varepsilon_z)/3$, $\theta = 3\varepsilon - \int_{T_0}^T \alpha(T) dT$, $s_i = \sigma_i - \sigma$, $e_i = \varepsilon_i - \varepsilon$,

G is the shear modulus, K is bulk modulus; is the relaxation core characterizing the decrease by the time t in shearing stresses caused by deformation at time t' the analytic record of which is non-exponential as in (2), at that, the parameters b and K_r are different from values used for determination of the structural parameter T_f ; $\alpha(T)$ is the thermal coefficient of linear expansion determined from the solution of the temperature problem according to formula (4).

The constitutive relations for the outer cylinder are written in line with the Prandtl-Reuss model with respect to thermal phenomena and division of small deformations into the convertible (elastic ε^e) and irreversible (plastic ε^p) components

$$\varepsilon_i = \varepsilon_i^e + \varepsilon_i^p. \quad (7)$$

The elastic state in stress space will be limited by the surface of limiting state of Mises and condition of active loading:

$$f(\sigma, T) = (\sigma_r - \sigma_\varphi)^2 + (\sigma_z - \sigma_\varphi)^2 + (\sigma_r - \sigma_z)^2 - 2\sigma_T^2(T) = 0$$

$$\frac{\partial f}{\partial \sigma_r} \dot{\sigma}_r + \frac{\partial f}{\partial \sigma_\varphi} \dot{\sigma}_\varphi + \frac{\partial f}{\partial \sigma_z} \dot{\sigma}_z + \frac{\partial f}{\partial T} \dot{T} > 0, \quad (8)$$

where maximum tensile stress $\sigma_T(T)$ depends only on temperature. The plastic components of the deformation tensor are determined in accordance with the law of associated flow:

$$\dot{\varepsilon}_r^p = \Lambda \frac{\partial f}{\partial \sigma_r}, \quad \dot{\varepsilon}_\varphi^p = \Lambda \frac{\partial f}{\partial \sigma_\varphi}, \quad \dot{\varepsilon}_z^p = \Lambda \frac{\partial f}{\partial \sigma_z}, \quad (9)$$

here, Λ has meaning of Langrangian multiplier while finding the maximum specific capacity of deformation with restriction (8).

Considering the relation (7) and the assumptions about the displacements the elastic deformations are rewritten as:

$$\varepsilon_r^e = \frac{\partial u}{\partial r} - \varepsilon_r^p, \quad \varepsilon_\varphi^e = \frac{u}{r} - \varepsilon_\varphi^p, \quad \varepsilon_z^e = \varepsilon_z - \varepsilon_z^p. \quad (10)$$

The boundary conditions are determined according to no-load conditions at the outer surfaces of the stem and equality of radial stresses and displacements when passing through the glass-metal boundary in case of perfect contact, without slippage along the cylinder axis ($\varepsilon_z^g = \varepsilon_z^m$):

$$u(R_1-, t) = u(R_1+, t), \quad \sigma_r(R_1-, t) = \sigma_r(R_1+, t),$$

$$\sigma_r(R_2, t) = 0, \quad (11)$$

$$\int_0^{R_1} \sigma_z(r, t) r dr + \int_{R_1}^{R_2} \sigma_z(r, t) r dr = 0.$$

Here R_1 radius of the glassy stem, $R_2 - R_1$ thickness of metal layer. Using the expressions (5)-(6), the displacement equation of equilibrium at $0 < r < R_1$:

$$\left(\frac{4}{3}G + K \right) \left(\frac{\partial^2 u}{\partial r^2} + \frac{1}{r} \frac{\partial u}{\partial r} - \frac{u}{r^2} \right) - \frac{2}{3}G \int_0^t M(t, t') \left(\frac{\partial^2 u}{\partial r^2} + \frac{1}{r} \frac{\partial u}{\partial r} - \frac{u}{r^2} \right) dt' = 0 \quad (12)$$

at the same time, for $R_1 < r < R_2$ with regard to (10) will be written as:

$$\frac{\partial^2 u}{\partial r^2} + \frac{1}{r} \frac{\partial u}{\partial r} - \frac{u}{r^2} = \frac{2G}{\frac{4}{3}G + K} \left(\frac{\partial(\varepsilon_r^p + \varepsilon_\varphi^p)}{\partial r} + \frac{\varepsilon_r^p - \varepsilon_\varphi^p}{r} \right). \quad (13)$$

When the plastic flow in the outer cylindrical layer is described by the Mises' equation of yielding (8) while the visco-elastic deformation, with consideration for the structural changes, is determined by the Kohlrausch relaxation core (2) and (5), at the moment, it seems to be impossible to achieve the analytic solution of the problem (5)-(13) even on the basis of all adopted simplifications. Based on the finite-difference method, the numerical analytic method of the problem is proposed in this paper.

Numerical-analytical method

The characteristic property of the problem (5)-(13) consists in its dependence on loading history, therefore, for numerical implementation, all equations were rewritten in small increments in time. The approximation of all defining relations with the use of the finite-difference method is accurately described, for example, in the work [23], therefore, we will highlight only distinctive features of the approach developed by authors in this paper.

In each temporal layer, the increments of displacements at $0 < r < R_1$ are written as the known coordinate functions, in which only the increment of integration constant $\Delta u^k = \Delta C_1^k \cdot r$ should be found. The increments of displacements at $R_1 < r < R_2$ are considered as the grid functions Δu_j^k , being determined from the system solution obtained as a result of finite-difference writing of equation (13). Herewith, the increment of constant ΔC_1^k can be found from solution of the consistent system resulting from the finite-difference presentation of equations (11) and (13). It is suggested to find the influence of the relaxation processes on the stresses in the form of the difference of the sums of the stress deviator components increments in all preceding time layers and "relaxation correcting" stress deviator components in the current layer.

When determining of the plastic deformations, the method of additional strains [24] is used, in which the iterative procedure of calculating the plastic deformation starts at each time step after the zero increments of stresses and strains are determined if the conditions (8) are met, when the plastic deformation "correcting" the stresses emerges.

With consideration for structural changes when passing through the glass transition phase and elastic-plastic stresses in the metal at (in) each time layer, under initial conditions of no increments of displacements, deformations and stresses, the calculation algorithm of combined visco-elastic stresses in the glass is:

1. When solving the temperature problem, the structural parameters (1)-(4) are determined:

$$T_f^k = T^0 + \sum_{k_1=1}^k \left(1 - \exp \left(- \left(\frac{(\xi^k - \xi^{k_1}) K_{rs}}{\eta_r} \right)^{b_s} \right) \right) \Delta T^k,$$

$$\xi^k = \xi^{k-1} + \sum_{k_1=1}^k \frac{\eta_r \Delta t}{\eta^{k_1-1}},$$

$$\lg \eta^k = \lg \eta^0 + B_e \left((T_f^k)^{-1} - (T^0)^{-1} \right) + B_f \left((T^k)^{-1} - (T_f^k)^{-1} \right),$$

$$\alpha^k = \alpha_e + (\alpha_f - \alpha_e) \frac{\Delta T_f^k}{\Delta T^k}.$$

2. The displacements in the region $0 < r < R_1$ are determined as solutions of the Euler equation, which is a consequence of the integro-differential equation (12), provided that the relaxation core (2) is independent on the r :

$$\Delta u_j^k = \Delta C^k r_j;$$

at $R_1 \leq r \leq R_2$ the displacement increments are determined from the system:

$$\begin{aligned} & \left(\frac{\Delta r_m}{2r_j} + 1 \right) \Delta u_{j+1}^k - \left(\frac{\Delta r_m^2}{r_j^2} + 2 \right) \Delta u_j^k + \left(1 - \frac{\Delta r_m}{2r_j} \right) \Delta u_{j-1}^k = \\ & = \frac{2G_m \Delta r_m^2}{4/3 G_m + K_m} \left(\frac{\Delta \varepsilon_{r_{j+1}}^{pk-1} - \Delta \varepsilon_{r_{j-1}}^{pk-1}}{2\Delta r_m} + \frac{\Delta \varepsilon_{r_j}^{pk-1} - \Delta \varepsilon_{\varphi_j}^{pk-1}}{r_j} \right), \end{aligned}$$

in general, at each temporal layer the displacements in the whole area are determined as

$$u_j^k = u_j^{k-1} + \Delta u_j^k$$

3. Determination of the stress increments is carried out using an iterative procedure that should contain at least two iterations: at the zero step for finding the increments ΔC_j^k , Δu_j^k , $\Delta \varepsilon_z^k$ the system (11) and (13) is solved in finite difference approximation, and at the interface of the layers the condition of continuity of displacements are written as

$$\Delta C^k = \frac{\Delta u_{j_0}^k}{J_0 \Delta r_g}$$

here $J_0 \Delta r_g$ – layer interface. After determining the displacement and stress increments using finite-difference analogues (5) and (6) as

$$\Delta \sigma_r^k = \Delta \sigma_\varphi^k = \left(\frac{2}{3} G_g + 6K_g \right) \Delta C^k + \left(3K_g - \frac{2}{3} G_g \right) \Delta \varepsilon_z^k - 3K_g \Delta \tilde{\alpha}_g^k, \quad (14)$$

$$\Delta \sigma_z^k = 2 \left(3K_g - \frac{2}{3} G_g \right) \Delta C^k + \left(3K_g + \frac{2}{3} G_g \right) \Delta \varepsilon_z^k - 3K_g \Delta \tilde{\alpha}_g^k,$$

we determine the increments of the stress deviator components and calculate the correction part that takes into account the mechanical relaxation in the layer

$$\Delta S_r^k = \frac{2}{3} \Delta \sigma_{rj}^k - \frac{1}{3} (\Delta \sigma_{\varphi j}^k + \Delta \sigma_{zj}^k), \quad \Delta S_\varphi^k = \frac{2}{3} \Delta \sigma_{\varphi j}^k - \frac{1}{3} (\Delta \sigma_{rj}^k + \Delta \sigma_{zj}^k),$$

$$\Delta S_r^k = \frac{2}{3} \Delta \sigma_{zj}^k - \frac{1}{3} (\Delta \sigma_{\varphi j}^k + \Delta \sigma_{rj}^k),$$

$$\Delta S_{cor,i}^k = \sum_{k_1=1}^{k-1} \left(1 - e^{-\left(\left(\frac{(\xi^k - \xi^{k_1}) K_{r\sigma}}{\eta_r} \right)^{b\sigma} \right)} \right) \Delta S_i^{k_1} - \sum_{k_1=1}^{k-2} \left(1 - e^{-\left(\left(\frac{(\xi^{k-1} - \xi^{k_1}) K_{r\sigma}}{\eta_r} \right)^{b\sigma} \right)} \right) \Delta S_i^{k_1},$$

$$\Delta S_i^k = \Delta S_i^k - \Delta S_{cor,i}^k \Delta C_j^k$$

here $\Delta \tilde{\alpha}_g^k = \alpha_g^k \cdot \Delta T$, $\alpha_g^k = \alpha_g(T^k)$.

At the next iteration, with consideration of the corrected deviatoric part of the stresses, we redefine the Δu_j^k , $\Delta \varepsilon_z^k$ from the repeated solution of the finite-difference analog of the system (11) and (13). We redefine the stress increments $0 \leq r \leq R_1$ with the use of formulas (14) and for $R_1 \leq r \leq R_2$ as

$$\Delta \sigma_{rj}^k = \left(\frac{4}{3} G_m + 3K_m \right) \frac{\Delta u_{j+1}^k - \Delta u_{j-1}^k}{2\Delta r_m} + \left(3K_m - \frac{2}{3} G_m \right) \left(\frac{\Delta u_j^k}{r_j} + \Delta \varepsilon_z^k \right) - 3K_m \Delta \tilde{\alpha}_m^k - 2G_m \Delta \varepsilon_{rj}^{pk},$$

$$\Delta \sigma_{\varphi j}^k = \left(\frac{4}{3} G_m + 3K_m \right) \frac{\Delta u_j^k}{r_j} + \left(3K_m - \frac{2}{3} G_m \right) \left(\frac{\Delta u_{j+1}^k - \Delta u_{j-1}^k}{2\Delta r_m} + \Delta \varepsilon_z^k \right) - 3K_m \Delta \tilde{\alpha}_m^k - 2G_m \Delta \varepsilon_{\varphi j}^{pk},$$

$$\Delta\sigma_{zj}^k = \left(\frac{4}{3}G_m + 3K_m \right) \Delta\varepsilon_z^k + \left(3K_m - \frac{2}{3}G_m \right) \left(\frac{\Delta u_{j+1}^k - \Delta u_{j-1}^k}{2\Delta r_m} + \frac{\Delta u_j^k}{r_j} \right) - 3K_m \Delta\tilde{\alpha}_m^k - 2G_m \Delta\varepsilon_{zj}^{pk},$$

where $\Delta\tilde{\alpha}_m^k = \alpha_m^k \cdot \Delta T$, $\alpha_m^k = \alpha_m(T^k)$, j - coordinate step number.

4. The increment of plastic deformation is calculated by method of additional deformations [23-24], if the stresses at k -th step satisfy the conditions (8) in time then in the process of additional iterations: at $0 \leq r \leq R_1$ let's specify ΔC^k , $\Delta\varepsilon_z^k$ are improved and the stress increments are redefined according to the algorithm described in step 3 for every iteration; at $R_1 \leq r \leq R_2$, at the zero step of iteration, the increment of the plastic deformation intensity $\Delta\varepsilon_i^P$ is defined as:

$$\Delta\varepsilon_{ij}^{p0} = \frac{\sqrt{2}}{3} \sqrt{(\Delta\varepsilon_{rj}^0 - \Delta\varepsilon_{\phi j}^0)^2 + (\Delta\varepsilon_{\phi j}^0 - \Delta\varepsilon_{zj}^0)^2 + (\Delta\varepsilon_{rj}^0 - \Delta\varepsilon_{zj}^0)^2},$$

where

$$\Delta\varepsilon_{rj}^0 = \frac{\frac{2}{3}\Delta\sigma_{rj}^0 - \frac{1}{3}(\Delta\sigma_{\phi j}^0 + \Delta\sigma_{zj}^0)}{2G_m}, \quad \Delta\varepsilon_{\phi j}^0 = \frac{\frac{2}{3}\Delta\sigma_{\phi j}^0 - \frac{1}{3}(\Delta\sigma_{rj}^0 + \Delta\sigma_{zj}^0)}{2G_m},$$

$$\Delta\varepsilon_{zj}^0 = \frac{\frac{2}{3}\Delta\sigma_{zj}^0 - \frac{1}{3}(\Delta\sigma_{\phi j}^0 + \Delta\sigma_{rj}^0)}{2G_m},$$

then the increment of the plastic deformations are determined as

$$\Delta\varepsilon_{rj}^{p0} = \frac{3\Delta\varepsilon_{ij}^{p0}}{2\sigma_T} \left(\frac{2}{3}\Delta\sigma_{rj}^0 - \frac{1}{3}(\Delta\sigma_{\phi j}^0 + \Delta\sigma_{zj}^0) \right),$$

$$\Delta\varepsilon_{\phi j}^{p0} = \frac{3\Delta\varepsilon_{ij}^{p0}}{2\sigma_T} \left(\frac{2}{3}\Delta\sigma_{\phi j}^0 - \frac{1}{3}(\Delta\sigma_{rj}^0 + \Delta\sigma_{zj}^0) \right),$$

$$\Delta\varepsilon_{zj}^{p0} = \frac{3\Delta\varepsilon_{ij}^{p0}}{2\sigma_T} \left(\frac{2}{3}\Delta\sigma_{zj}^0 - \frac{1}{3}(\Delta\sigma_{\phi j}^0 + \Delta\sigma_{rj}^0) \right).$$

Determined $\Delta\varepsilon_{rj}^{p0}$, $\Delta\varepsilon_{\phi j}^{p0}$, $\Delta\varepsilon_{zj}^{p0}$ are inserted into the equations of the previous steps 2 and 3 and the increments of displacements are determined, and the stresses are redefined. Further, the iterative process of calculating the deformation increments is performed:

$$\Delta\varepsilon_{rj}^{p1} = \frac{3\Delta\varepsilon_{ij}^{p0}}{2\sigma_T} \left(\frac{2}{3}\Delta\sigma_{rj}^1 - \frac{1}{3}(\Delta\sigma_{\phi j}^1 + \Delta\sigma_{zj}^1) \right),$$

$$\Delta\varepsilon_{\phi j}^{p1} = \frac{3\Delta\varepsilon_{ij}^{p0}}{2\sigma_T} \left(\frac{2}{3}\Delta\sigma_{\phi j}^1 - \frac{1}{3}(\Delta\sigma_{rj}^1 + \Delta\sigma_{zj}^1) \right),$$

$$\Delta\varepsilon_{zj}^{p1} = \frac{3\Delta\varepsilon_{ij}^{p0}}{2\sigma_T} \left(\frac{2}{3}\Delta\sigma_{zj}^1 - \frac{1}{3}(\Delta\sigma_{\phi j}^1 + \Delta\sigma_{rj}^1) \right),$$

$$\Delta\varepsilon_{ij}^{p1} = \frac{\sqrt{2}}{3} \sqrt{(\Delta\varepsilon_{rj}^{p1} - \Delta\varepsilon_{\phi j}^{p1})^2 + (\Delta\varepsilon_{\phi j}^{p1} - \Delta\varepsilon_{zj}^{p1})^2 + (\Delta\varepsilon_{rj}^{p1} - \Delta\varepsilon_{zj}^{p1})^2}.$$

The iterative process is ceased subject to the condition: $\frac{|u_j^l - u_j^{l-1}|}{|u_j^l|} \leq \varepsilon$,

the transition to the next time layer takes place (ε is the prescribed accuracy).

Calculation results

When investigating different modes of annealing, the following data were used for borosilicate glass [25]: $\eta_0 = 10^{4.25}$ MPa·s; $B_e = 28726.85$ °C; $B_f = 13726.85$ °C; $K_{rs} = 10^{10.7}$; $b_s = 0.65$; $\eta_r = 10^3$ MPa·s; $\alpha_f = 52 \times 10^{-7}$ °C⁻¹; $\alpha_e = 210 \times 10^{-7}$ °C⁻¹; $K_{r\sigma} = 10^{4.7}$; $b_\sigma = 0.5$; $G_g = 0.24 \times 10^5$ MPa; $K_g = 0.4 \times 10^5$ MPa; $\alpha_m = 115 \times 10^{-7}$ °C⁻¹; $G_m = 0.81 \times 10^5$ MPa; $K_m = 1.75 \times 10^5$ MPa. The calculations when solving the temperature part of the problem have shown that the characteristic change in the fictitious temperature during cooling and heating up (Fig. 2) allows us to determine the boundaries of the glass transition interval as temperatures at which the rates of change of the fictitious temperature by temperature begin to differ from 0 and 1, which means, respectively, the difference from glass in the frozen state and equilibrium melt, which is reflected respectively in the changes in the thermal coefficient of linear expansion and viscosity (Fig. 3)

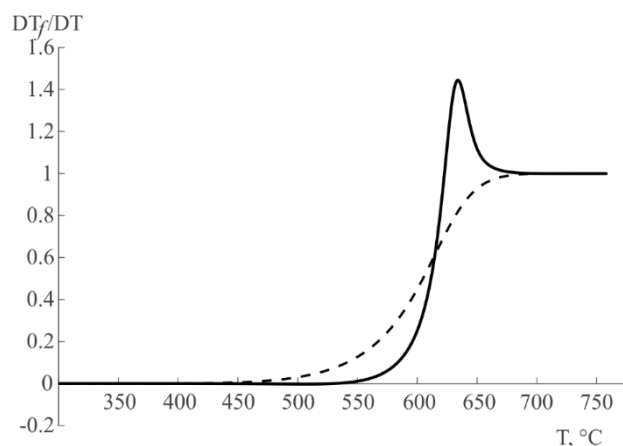


Fig. 2. Characteristic change in the fictitious temperature during cooling and heating up

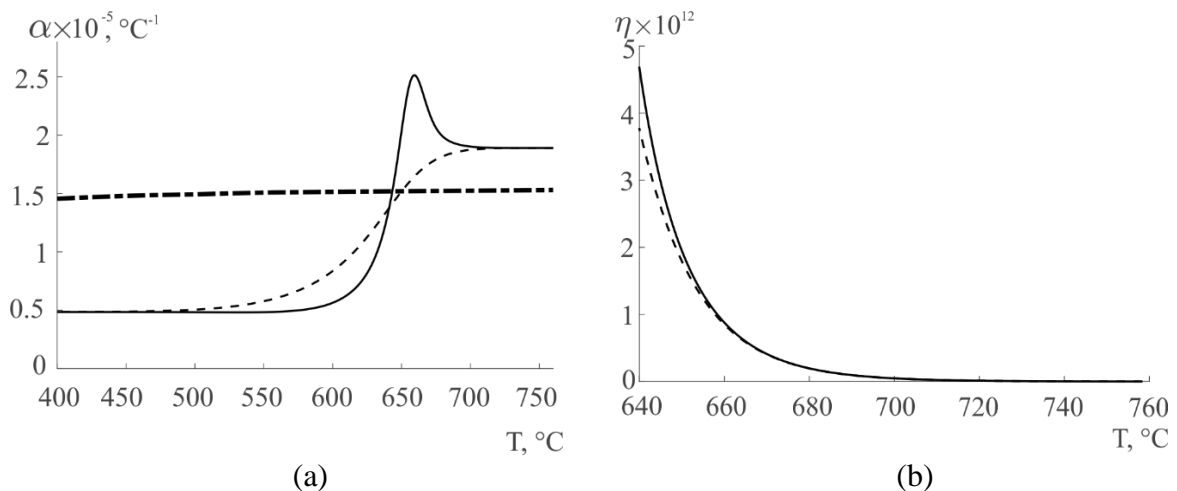


Fig. 3. Temperature dependence of the thermal coefficient of linear expansion (a) and viscosity (b): - heating up, -- cooling; -·-· thermal coefficient of linear expansion of the metal

In Figure 3(a) it is possible to identify the temperature at which the graphs of thermal coefficients of linear expansion of glass and metal on heating up and cooling have points of intersection for certain mode. At this temperature the stress in the soldered joint changes the sign, for flat soldered joints [19–20] it is accepted to choose the cooling rate (q_3) in the area

between the upper temperature of annealing and the intersection point of graphs of thermal coefficients of linear expansion of glass and metal, as much as possible reduced at least by the increase of compressive stresses.

The following Figs. 4-5 show graphs of stress changes as a function of temperature in the 1st layer (glass) and at the interface between the layers in the 2nd layer (metal), the beginning of the process was assumed as cooling after obtaining the soldered joint from 650 °C (1st stage at a constant rate $q_1 = 3$ °C/min), then annealing was carried out according to the scheme of stage 2 - heating up to the annealing temperature (after pre-calculations, a temperature of 560 °C was taken), exposure at 560 °C for 2 h and cooling; $q_2 = q_3 = q_4 = 3$ °C/min.

From the graphs in Fig. 4, the temperature range and the stress level at which plastic flow develops in the 2nd layer is noticeable; on the graph of the intensity change at all stages in this interval, the graphs merge and correspond to the graph of the change in the yield stress (Fig. 4, lower right graph).

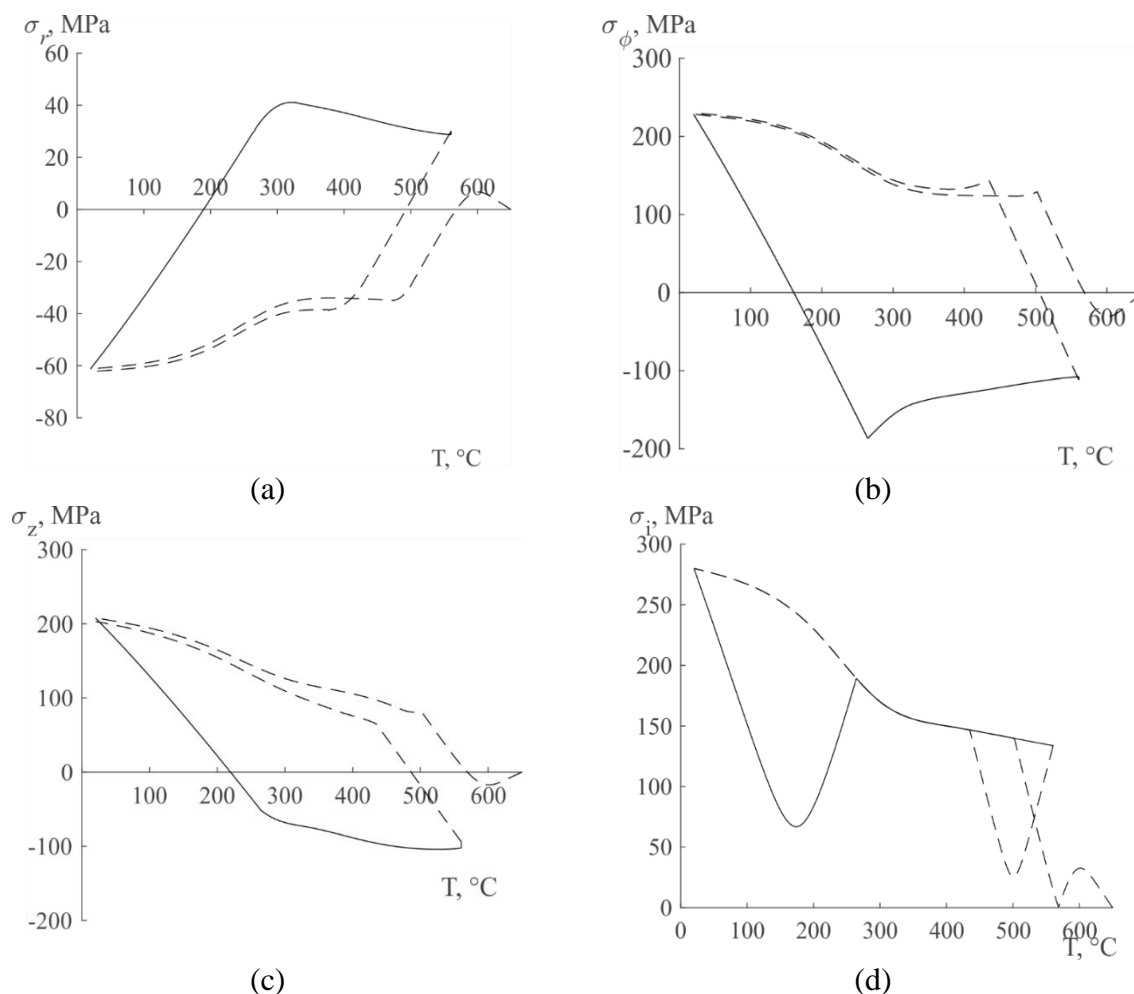


Fig. 4. Change of stress and intensity in the 2nd layer (metal) at the interface of the connection with the glass: (a) $\sigma_r(T)$; (b) $\sigma_\phi(T)$; (c) $\sigma_z(T)$; (d) $\sigma_i(T)$

In the graphs of stress changes in the 1st layer (glass) (Fig. 5) it is noticeable that after cooling during annealing the stress level changes (highlighted area in σ_z) and is controlled not only by annealing but also by the cooling rate after exposure. It is proved that the stress level and the value of exposure, besides the cooling rate, are also influenced by the heating rate (Figs. 5 and 6). Let's note that such effects are not revealed either at analytical solution for the case of simple Maxwell type cores, or moreover at elastic approximation.

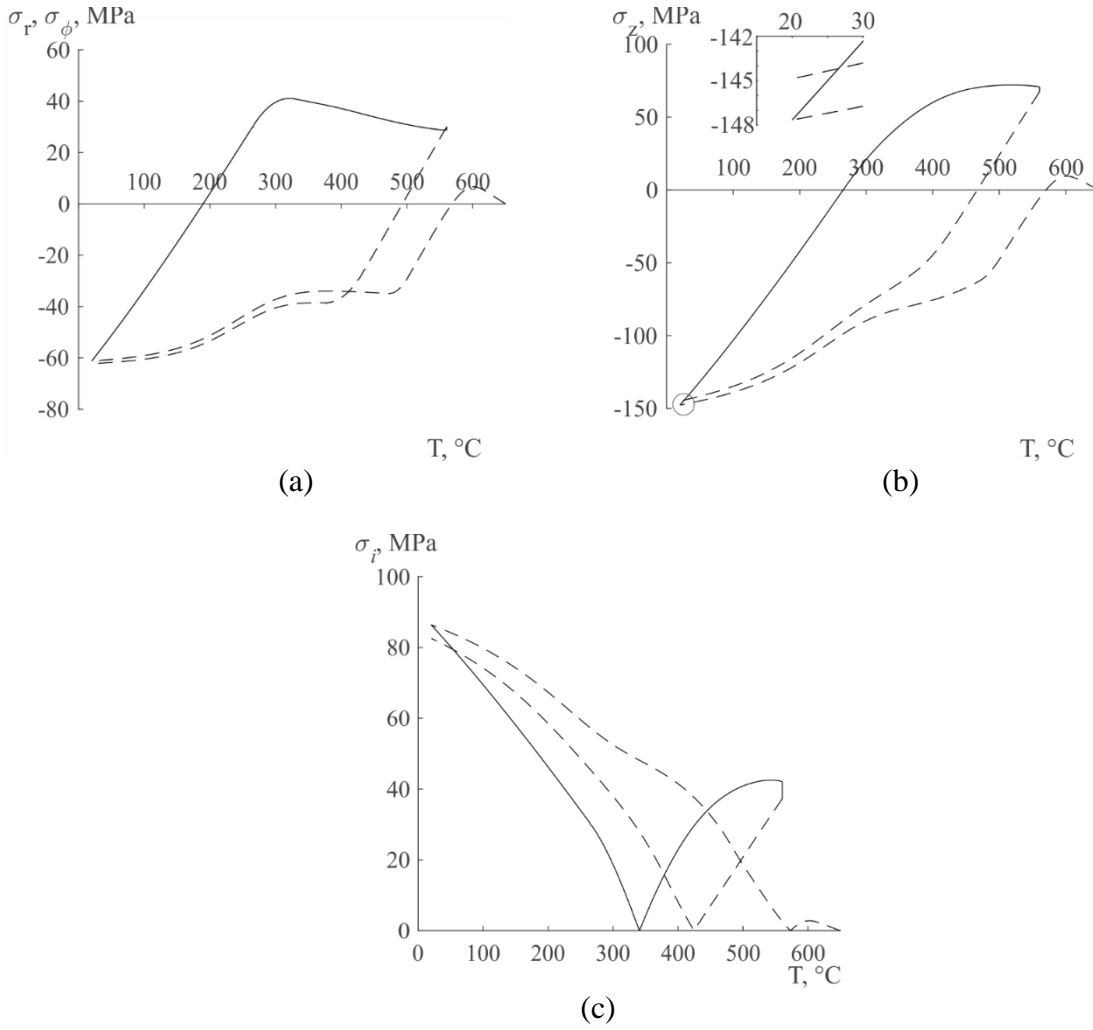


Fig. 5. Change of stress and intensity in the 1st layer (glass):
 (a) $\sigma_r(T)$ и $\sigma_{\phi}(T)$; (b) $\sigma_z(T)$; (c) $\sigma_i(T)$

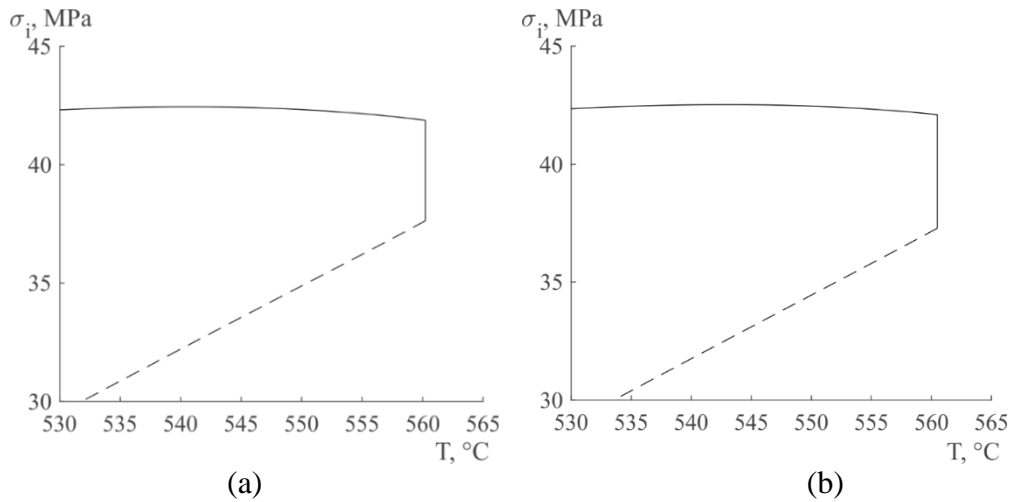


Fig. 6. Fragments of graphs for the layer (1) in the area of exposure at the heating rate $q_1 = 10 \text{ }^{\circ}\text{C}/\text{min}$ and cooling at $q_3 = q_4 = 1,5 \text{ }^{\circ}\text{C}/\text{min}$ (a), at $q_3 = q_4 = 3 \text{ }^{\circ}\text{C}/\text{min}$ (b)

Conclusion

The problem of determining the change in parameters of the strenuously-deformed state in the two-layer cylindrical glass-metal composite in the course of annealing with consideration for glass transition process in the inner glass layer and plastic deformation of the outer metal layer was set and solved. The algorithm of calculation of the cylindrical vitrified layer connected to the plastically deformed non-vitrified layer was proposed. The calculations in accordance with the proposed algorithm allow us to determine the technological stresses with consideration for structural and mechanical relaxation processes. The numerical method suggested in the paper can be applied to the case of several vitrified cylindrical layers.

References

1. Sergi R, Bellucci D, Cannillo, V. A Comprehensive Review of Bioactive Glass Coatings: State of the Art, Challenges and Future Perspectives. *Coatings*. 2020;10: 757.
2. Thiyagarajan R, Senthil Kumar M. Enhanced energy absorption and microstructural studies on hollow glass microsphere filled closed cell aluminum matrix syntactic foam. *Proceedings of the Institution of Mechanical Engineers, Part C: Journal of Mechanical Engineering Science*. 2022;237(8): 1887–1900.
3. Mingming Su, Han Wang, Hai Hao, Thomas Fiedler. Compressive properties of expanded glass and alumina hollow spheres hybrid reinforced aluminum matrix syntactic foams. *Journal of Alloys and Compounds*. 2020;821: 153233.
4. Caprino G, Lopresto V, Iaccarino P. A simple mechanistic model to predict the macroscopic response of fibreglass–aluminium laminates under low-velocity impact. *Composites Part A: Applied Science and Manufacturing*. 2007;38: 290–300.
5. Boussu F, Provost B, Lefebvre M, Coutellier D. New textile composite solutions for armouring of vehicles. *Adv. Mater. Sci. Eng.* 2019;2019: 7938720. 2019.
6. Karpov EV, Demeshkin AG. Strain and fracture of glass-fiber laminate containing metal layers. *J. Appl. Mech. Tech. Physics*. 2018;59(4): 699–705.
7. Pikul' VV. *Efficiency of glass-metal composite*. Moscow: Perspektivnyye materialy; 2000. (In-Russian)
8. Lyubimova ON, Dryuk SA. Simulation parameters of temperature in the process of manufacturing a glass-metal composite. *Thermophysics and Aeromechanics*. 2017;24(1): 125–133.
9. James PF, Chen M, Jones FR. Strengthening of soda-lime silica glass by sol-gel – and melt-derived coatings. *Journal of Non-Crystalline Solids*. 1993;155(2): 99–109.
10. Lyubimova ON, Morkovin AV, Dryuk SA, Nikiforov PA. Structure and constitution of glass and steel compound in glass-metal composite. *AIP Conference Proceedings*. 2014;1623: 379–382.
11. Tropin TV, Schmelzer JW, Aksenov VL. Modern aspects of the kinetic theory of glass transition. *Physics-Uspekhi*. 2016;59: 42–66.
12. Schmelzer J.W.P. Kinetic criteria of glass formation and the pressure dependence of the glass transition temperature. *J. Chem. Phys.* 2012;136: 074512.
13. Startsev YK. Phenomenological description of the glass transition and structural relaxation processes. In: *Vol 7 Physical and chemical aspects of studying clusters, nanostructures and nanomaterials*. Tver': Tver. gos. un-t; 2015. p.494–504. (In-Russian)
14. Tool AQ. Relation between inelastic deformability and thermal expansion of glass in its annealing range. *J. Am. Ceram. Soc.* 1946;29(9): 240–253.
15. Narayanaswami OS. A model of structural relaxation in glass. *J. Am. Ceram. Soc.* 1971;54(10): 491–498.

16. Moynihan CT, Macedo PB, Montrose CJ, Montrose CJ, Gupta PK, DeBolt MA, Dill JF, Dom BE, Drake PW, Eastal AJ, Elterman PB, Moeller RP, Sasabe H, Wilder JA. Structural relaxation in vitreous material. *Ann. New York Acad. Sci.* 1976;279: 15–35.
17. Ojovan MI, Tournier RF. On structural rearrangements near the glass transition temperature in amorphous silica. *Mater.* 2021;14(18): 5235.
18. Mazurin OV. *Glass transition*. Lenindrad: Nauka; 1986. (In-Russian)
19. Mazurin OV. *Annealing of glass-to-metal junctions*. Leningrad: Energia; 1980. (In-Russian)
20. Gonchukova NO. Calculation of stresses in amorphous nickel–phosphorus coatings on metallic substrates. *Glass Physics and Chemistry*. 2004;8(1): 356–358.
21. Kalgin AV. Structural relaxation in an amorphous phase of the thin-film nanogranular composite (x)Ni – (1–x)PNBZT. *Ferroelectrics*. 2020; 561: 1–11.
22. Lybimova ON, Barbotko MA. Modeling of heat transfer due to induction heating of laminated glass-metal materials. *Thermophysics and Aeromechanics*. 2021;28: 87102.
23. Bartenev GM, Sanditov DS. *Relaxation processes in glassy systems*. Novosibirsk: Nauka; 1986. (In-Russian)
24. Galanin MP, Guzev MA, Nizkaya TV. *Numerical solution of the thermoplasticity problem with additional state parameters*. To be published in: *Inst. Appl. Math.* [Preprint] 2007. Available from: https://keldysh.ru/papers/2007/rep08/rep2007_08.html [Accessed 1th June 2023].
25. Rodriguez-Tinoco C, Gonzalez-Silveira M, Ramos MA, Rodriguez-Viejo J. Ultrastable glasses: new perspectives for an old problem. *Riv. Nuovo Cim.* 2022;45: 325–406.

THE AUTHORS

Barbotko M.A.

e-mail: barbotko_ma@dvfu.ru

Lyubimova O.N. 

e-mail: berms@mail.ru

Ostanin M.V. 

e-mail: maximostanin91@yandex.ru